ELSEVIER

Brain Research 815 (1999) 154–166

BRAIN RESEARCH INTERACTIVE

Interactive report

Neurons of the rat suprachiasmatic nucleus show a circadian rhythm in membrane properties that is lost during prolonged whole-cell recording [1]

Jeroen Schaap [a,*], Nico P.A. Bos [b], Marcel T.G. de Jeu [b], Alwin M.S. Geurtsen [b], Johanna H. Meijer [a], Cyriel M.A. Pennartz [b]

[a] *Dept. of Physiology, Leiden Universitair Medisch Centrum, Rijksuniversiteit Leiden, P.O. Box 9604, 2300 RC Leiden, The Netherlands*
[b] *Netherlands Institute for Brain Research, Meibergdreef 33, 1105 AZ Amsterdam, The Netherlands*

Accepted 22 September 1998

Abstract

The suprachiasmatic nucleus is commonly considered to contain the main pacemaker of behavioral and hormonal circadian rhythms. Using whole-cell patch-clamp recordings, the membrane properties of suprachiasmatic nucleus neurons were investigated in order to get more insight in membrane physiological mechanisms underlying the circadian rhythm in firing activity. Circadian rhythmicity could not be detected either in spontaneous firing rate or in other membrane properties when whole-cell measurements were made following an initial phase shortly after membrane rupture. However, this apparent lack of rhythmicity was not due to an unhealthy slice preparation or to seal formation, as a clear day/night difference in firing rate was found in cell-attached recordings. Furthermore, in a subsequent series of whole-cell recordings, membrane properties were assessed directly after membrane rupture, and in this series we did find a significant day/night difference in spontaneous firing rate, input resistance and frequency adaptation. As concerns the participation of different subpopulations of suprachiasmatic nucleus neurons expressing circadian rhythmicity, cluster I neurons exhibited strong rhythmicity, whereas no day/night differences were found in cluster II neurons. Vasopressin-containing cells form a subpopulation of cluster I neurons and showed a more pronounced circadian rhythmicity than the total population of cluster I neurons. In addition to their strong rhythm in spontaneous firing rate they also displayed a day/night difference in membrane potential.

Keywords: Suprachiasmatic nucleus; Circadian rhythms; Rat hypothalamic slice; Electrophysiology; Whole-cell recording

1. Introduction

The suprachiasmatic nucleus (SCN), situated in the ventral hypothalamus, is considered to be the main pacemaker of circadian rhythms in mammals [16]. The most conclusive evidence gathered thus far consists of experiments showing that the endogenous rhythm of one animal can be imposed on another one by transplanting the SCN [25]. Because the spontaneous firing rate of SCN neurons serves as a direct marker of endogenous pacemaker activity, electrophysiological investigations play an important role in the elucidation of mechanisms underlying circadian rhythmicity of the SCN. Both in vivo and in vitro, SCN neurons show a circadian rhythm in their spontaneous firing activity, as they are active during the subjective day and relatively quiet during the subjective night. The circadian rhythm in spontaneous firing rate has been reported with the use of several extracellular techniques [7,8,18].

There is strong evidence to suggest that the circadian rhythm in firing rate is generated within individual neurons, in both vertebrate and invertebrate species. The first piece of evidence came from investigations on isolated retinal basal neurons from *Bulla gouldiana* [2]. Long-term intracellular recordings from isolated *Bulla* neurons in vitro show that the sustained circadian rhythm in firing rate was driven by a parallel change in membrane potential and membrane conductance [19]. More recently, extracellular recordings of SCN neurons cultured on multi-electrode plates showed that they are capable of maintaining an independently phased circadian rhythm in firing rate

* Corresponding author. Tel.: +31-71-5276811; Fax: +31-71-5276782; E-mail: J.Schaap@Physiology.MedFac.LeidenUniv.nl

[1] Published on the World Wide Web on 20 October 1998.

0006-8993/99/$ - see front matter
PII: S0006-8993(98)01025-7

Table 1
Overview of membrane properties measured in experiment 1: whole-cell recordings after a stabilization period

Property	CT 4–10	CT 12–24	*P*-value
SFR (Hz)	3.1±0.4	3.1±0.5	n.s.
Coefficient of variation	0.36±0.04	0.39±0.04	n.s.
MP (mV)	−56.1±1.1	−56.4±0.5	n.s.
R_{in} (GΩ)	1.34±0.07	1.25±0.06	n.s.
τ_m (ms)	29±2	28±2	n.s.
Adaptation rate (ms s^{-1})	33.1±10	59.5±25	n.s.
AHP_T (mV)	−7.4±0.9	−7.2±0.7	n.s.

The mean values are given ± s.e.m. The quantification of membrane properties is described in the methods section; *P*-values were calculated using Mann–Whitney's *U*-test. Sample sizes were 22 (CT 4–10) and 59 (CT 12–24), respectively. n.s.: not significant

[9,31], while earlier findings demonstrated circadian rhythmicity to be independent of action potential-driven synaptic transmission [4,28].

In addition to knowledge about patterns of spontaneous firing activity, investigations of membrane properties of SCN neurons are necessary in order to get more insight in the transduction of an intracellular and presumably molecular [6,30] rhythm into a circadian modulation of firing rate and associated homeostatic whole-body functions. Some basic knowledge is available about the electrophysiological properties of SCN neurons. Kim and Dudek [13] described the membrane properties of suprachiasmatic neurons in general terms without discrimination between circadian time points. Another sharp electrode study [1] described the properties of SCN neurons with a focus on the H-current that is expressed by virtually all SCN neurons. However, in whole-cell patch-clamp recordings it appeared later that the H-current is activated at membrane potentials too negative for this current to be of substantial importance for regulation of circadian rhythmicity [11]. In a previous study using whole-cell patch-clamp recordings, we distinguished three clusters of neurons in the SCN based on their membrane properties [22].

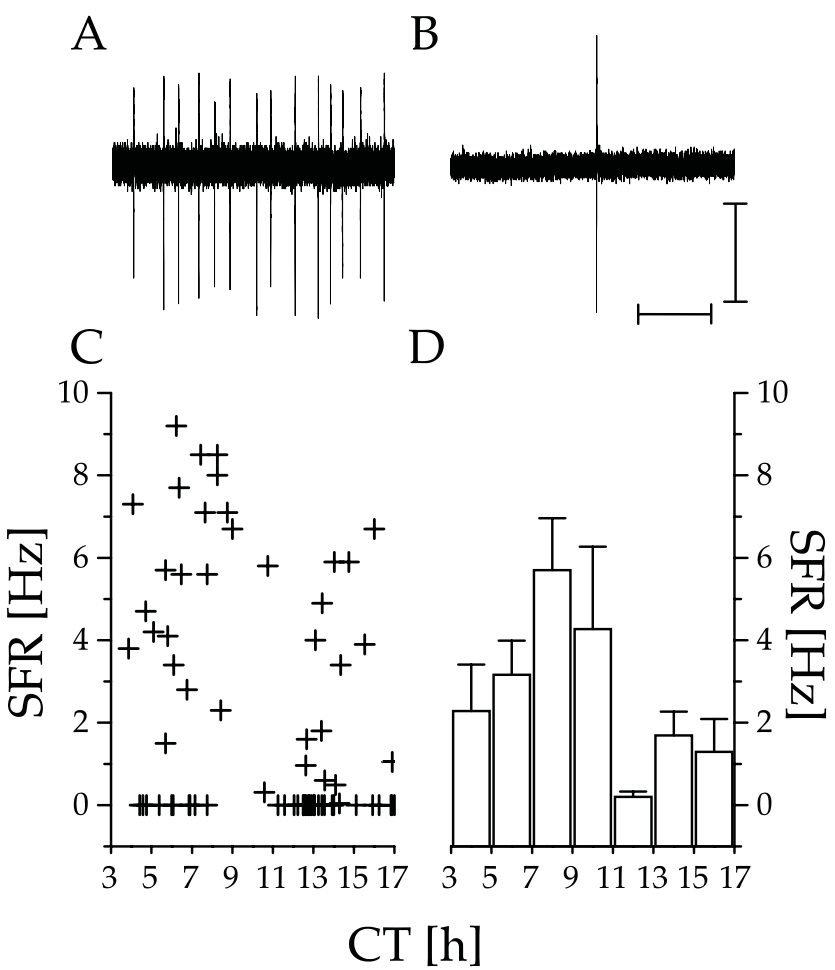

Fig. 1. Comparison of the spontaneous firing rate measured during subjective day versus night during experiment 2, cell-attached measurements. Examples of current traces at a holding potential of 0 mV are shown during (A) subjective day and (B) subjective night. Fast current transients reflecting spikes can clearly be discerned. Scale bars are 500 ms and 60 pA (A) or 40 pA (B). (C) The spontaneous firing rate of individual cells is plotted against circadian time and (D) is plotted against CT as rates averaged within bins of 2 h.

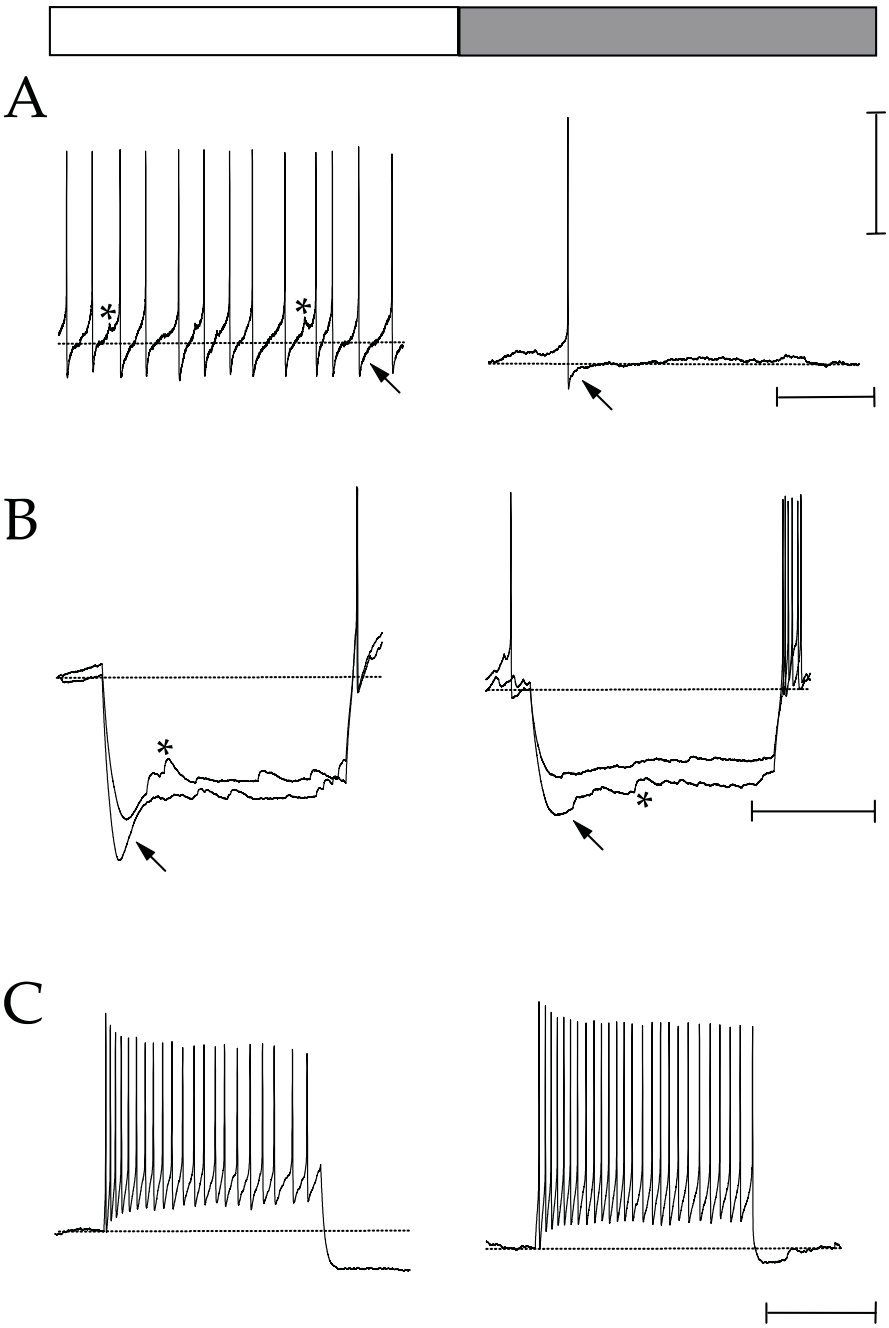

Fig. 2. Examples of whole-cell current-clamp recordings used to quantify membrane properties of SCN neurons during subjective day and night, from experiment 3: neurons measured immediately after membrane rupture. The traces in the left and right panels were recorded during subjective day and night, respectively, as is marked by the white and gray bars above the figures. All traces were from cluster I cells. In every trace a dotted line represents the basal membrane potential. (A) The uppermost traces are examples of spontaneous neuronal activity, with a firing rate of 7.8 Hz and basal membrane potential of −53 mV for the left panel; 2.0 Hz and −58 mV for the right panel. Note the irregular firing pattern, the steeply rising phase of the spike afterhyperpolarization (arrow) and the spontaneous postsynaptic potentials (asterisks). (B) Examples of voltage responses to hyperpolarizing current steps. Responses to current steps of −25 and −35 pA are shown, with values of 2.2 GΩ and −49 mV for input resistance and basal membrane potential of the cell in the left panel and 1.3 GΩ and −56 mV for the cell in the right panel. Note the steep response of the day-cell with subsequent larger time-dependent inward rectifier (arrow) and large spontaneous synaptic (presumably GABAergic) events (asterisk), whereas the night cell exhibited smaller voltage responses together with a more modest time-dependent inward rectification. (C) The lowermost panels present voltage responses to current steps of +40 pA. The evoked spike trains had a stronger frequency adaptation and deeper afterhyperpolarization as compared to the night phase. Adaptation rates and afterhyperpolarization were 46 ms s^{-1} and −13 mV (day, left) versus 25 ms s^{-1} and −5 mV (night, right). Scale bars denote 500 ms (*x*-axis) and 40 mV (*y*-axis).

In a patch-clamp study conducted in voltage-clamp mode, Jiang et al. [12] reported a weak circadian variation in membrane conductance and a more robust variation in holding current. However, the rhythm in membrane conductance was out of phase with the rhythm in holding current and with that in firing rate. Since these data stand, at least in part, in contrast to the results obtained in the *Bulla* model [2] we decided to perform a separate whole-cell patch-clamp study examining this issue.

The primary aim of the present study was to assess the possibility of measuring circadian rhythmicity in membrane properties with the whole-cell patch-clamp technique in current-clamp mode. In a first series of experiments, which focused on the time window following an initial, transitional phase associated with membrane rupture, no significant rhythmicity could be detected, suggesting that either our preparation or our recording methods were not suitable for recording circadian rhythmicity. In a second series these possibilities were further examined in cell-attached recordings. In this series a significant day/night difference in firing rate could be demonstrated, showing that circadian rhythmicity in our thin slice preparation was functionally preserved. In a third series, membrane properties of SCN neurons were again measured with the whole-cell method but now assessed directly after break-in, before intracellular dialysis was presumably completed. With the latter method, a circadian rhythm in several membrane properties was demonstrated in the total population of SCN neurons. When examining subpopulations of the SCN, we found that cluster I neurons (including vasopressin-positive cells) clearly contributed to the overall rhythm, while day/night differences could not be identified in cluster II cells.

2. Material and methods

2.1. Preparation of brain slices

Experimental procedures have been previously described by Pennartz et al. [22] and are in accordance with national and European guidelines on animal experiments. In short, male Wistar rats of four to seven weeks old were entrained for at least two weeks to a 12:12 light/dark regime. Two light/dark regimes were used, one starting at 07:00 AM for subjective day measurements and one starting at 23:00 PM for subjective night measurements, in order to keep both the actual time of recording and the delay between dissection and recording within the same range for subjective day and night. The animals were anesthetized during the day phase with 60 mg pentobarbital/kg i.p. (Nembutal, Sanofi Sante, The Netherlands) and transcardially perfused with cold artificial cerebrospinal fluid (aCSF), consisting of (mM) 124 NaCl, 26.2 $NaHCO_3$, 3.5 KCl, 1.0 NaH_2PO_4, 1.3 $MgSO_4$, 2.5 $CaCl_2$ and 10 D-glucose (Sigma), oxygenated with carbogen (5%

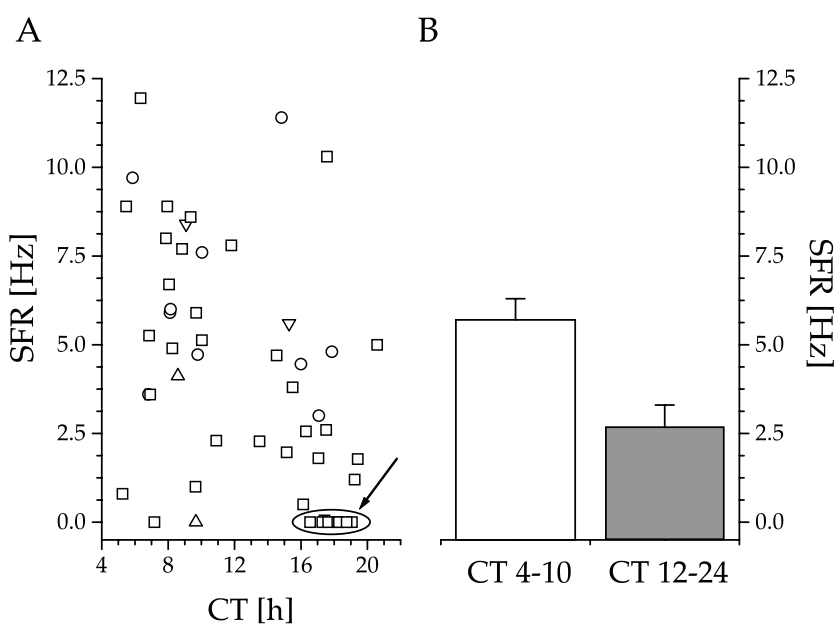

Fig. 3. Comparison of spontaneous firing rate (SFR) as measured during subjective day versus subjective night during experiment 3: whole-cell recordings measured immediately after membrane rupture. (A) SFR of individual cells is plotted against the estimated circadian time of the recording. Symbols label clusters; squares, cluster I ($n = 37$); circles, cluster II ($n = 9$); upward triangles, cluster III ($n = 2$); downward triangles, cases intermediate ($n = 2$). Clustering criteria can be found in the methods section, or more extensively in Ref. [22]. The encircled group of cells represent neurons ($n = 7$) that were silent during the subjective night, all of them belonging to cluster I. Note the relative high firing rates of cluster II cells at night. (B) Average spontaneous firing rate during subjective day, CT 4–10, and subjective night, CT 12–24. Error bars denote s.e.m.; for actual values see Table 2. Sample sizes were 25 neurons for both subjective day and night.

Table 2
Overview of membrane properties measured in experiment 3: Whole-cell recordings immediately after membrane rupture

Property	CT 4–10	CT 12–24	*P*-value
SFR (Hz)	5.3 ± 0.6	2.6 ± 0.6	$P < 0.001$
Coefficient of variation	0.39 ± 0.07	0.57 ± 0.08	$P < 0.05$
MP (mV)	-54.3 ± 1.1	-56.2 ± 0.8	n.s.
R_{in} (GΩ)	1.8 ± 0.2	1.0 ± 0.1	$P < 0.001$
τ_m (ms)	40 ± 3	30 ± 3	$P < 0.05$
Adaptation rate (ms s^{-1})	35 ± 4	19 ± 4	$P < 0.05$
AHP_T (mV)	-9 ± 1	-4 ± 1	$P < 0.05$
Frequency during evoked spike trains (Hz)	24 ± 3	27 ± 5	n.s.

The mean values are given ± s.e.m. The quantification of membrane properties is described in the methods section; *P*-values were calculated using Mann Whitney's U-test. Sample sizes were 25 (CT 4–10) and 25 (CT 12–24), respectively. n.s.: not significant.

CO_2, 95% O_2). The brain was removed from the skull and trimmed to a block containing the hypothalamus. From this block two or three 200 μm thick transversal slices containing the SCN were cut using a vibroslicer (Campden Instruments, UK), while this block was immersed in cold aCSF. The slices were kept at room temperature in oxygenated aCSF until they were transferred to the recording chamber. Prepared brain slices were stored for at least one hour before measurements were started. In the recording chamber slices were kept submerged and superfused with oxygenated aCSF at a rate of 2–3 ml/min at 33°C.

2.2. Whole-cell recordings

Slices were inspected visually with an upright Axioscope microscope (Zeiss, Germany) equipped with an objective (40×) with Hoffman modulation contrast. From slices with a clearly visible suprachiasmatic nucleus cells in a position at least 25 μm, but generally 50–100 μm below the slice surface, and sampled throughout the SCN, were chosen to record from. Pipettes were filled with a HEPES-buffered gluconate solution (Experiments 1 and 2 (mM): 135 KGluconate, 10 KCl, 10 HEPES, 1 EGTA and 2.0 Na_2ATP; pH 7.4; osmolarity 270–275 mOsm/kg; Experiment 3: idem, but without ATP). The pipette resistance ranged from 5 to 8 MΩ. While the pipette was moving through the slice, slight positive pressure was applied to keep the pipette tip clean. When a cell membrane was reached the positive pressure was removed and negative pressure was applied, resulting in a gigaseal. Measurements were only continued when the seal resistance was larger than 2 GΩ for whole-cell recordings or in

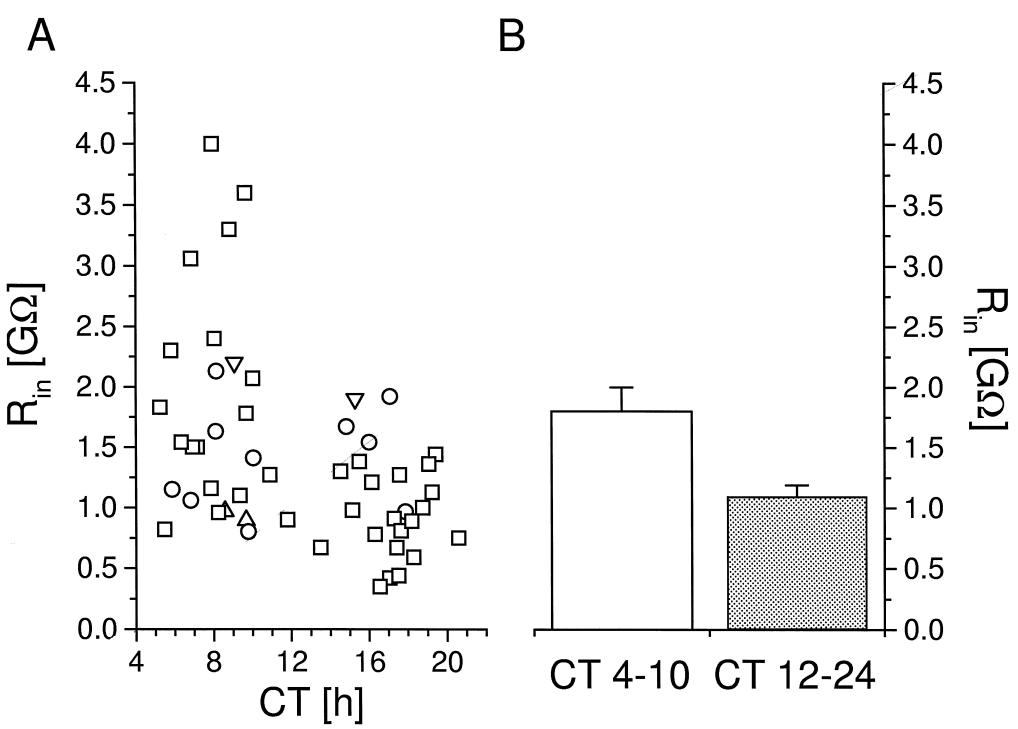

Fig. 4. Comparison of input resistance measured during subjective day versus night during experiment 3: whole-cell recordings measured immediately after membrane rupture. Plotting conventions are identical to those of Fig. 3 (squares, cluster I; circles, cluster II; upward triangles, cluster III; downward triangles, intermediate cases). In (A) the input resistance, R_{in}, of the individual neurons and in (B) the average values are given.

excess of 30 MΩ for cell-attached recordings. Seal resistances clearly below 1 GΩ can be considered to produce loose-patch-recordings [23]. Membrane currents and potentials were recorded on setups equipped with either an Axopatch 1D or Axoclamp 2B amplifier and stored by PC computers running the PClamp 6 software suite (amplifiers and software from Axon Instruments, USA). Current clamp traces obtained in Experiments 1 and 3 were not filtered while the voltage clamp traces in Experiment 2 were low-pass filtered with a cut-off frequency of 2 or 5 kHz.

Below, we present results from three different series of experiments which were conducted according to the following procedures. In the first series the membrane under a sealed pipette tip was ruptured by negative pressure in order to gain direct access to the cell interior. The cell was then allowed to stabilize for about 10 min in current-clamp mode. Subsequently the electrophysiological properties of the cell were determined. The firing behavior of the cells was measured for at least one minute in the absence of current injection. These recordings provided data about the spontaneous firing rate (SFR), the coefficient of variation of spike intervals, the spike waveform and basal membrane potential (MP). MP was determined from the low-pass read-out of the amplifier and subsequently corrected for the junction potential (−13 mV). Depolarizing and hyperpolarizing current steps (1000 ms in incremental steps of 3–5 pA) were applied in order to assess the input resistance (R_{in}), the membrane time constant (τ_m), the presence of low threshold Ca^{2+} potentials, frequency adaptation and the spike-train afterhyperpolarization (AHP_T) [22]. Using these parameters, cells were grouped into clusters (see below).

In the second series spontaneous firing behavior was measured in cell-attached mode. After obtaining a seal the SFR was assessed by monitoring fast current transients reflecting spikes at a holding potential of 0 mV. Current traces were recorded for at least one minute. Traces with unstable holding current or SFR were excluded from anal-

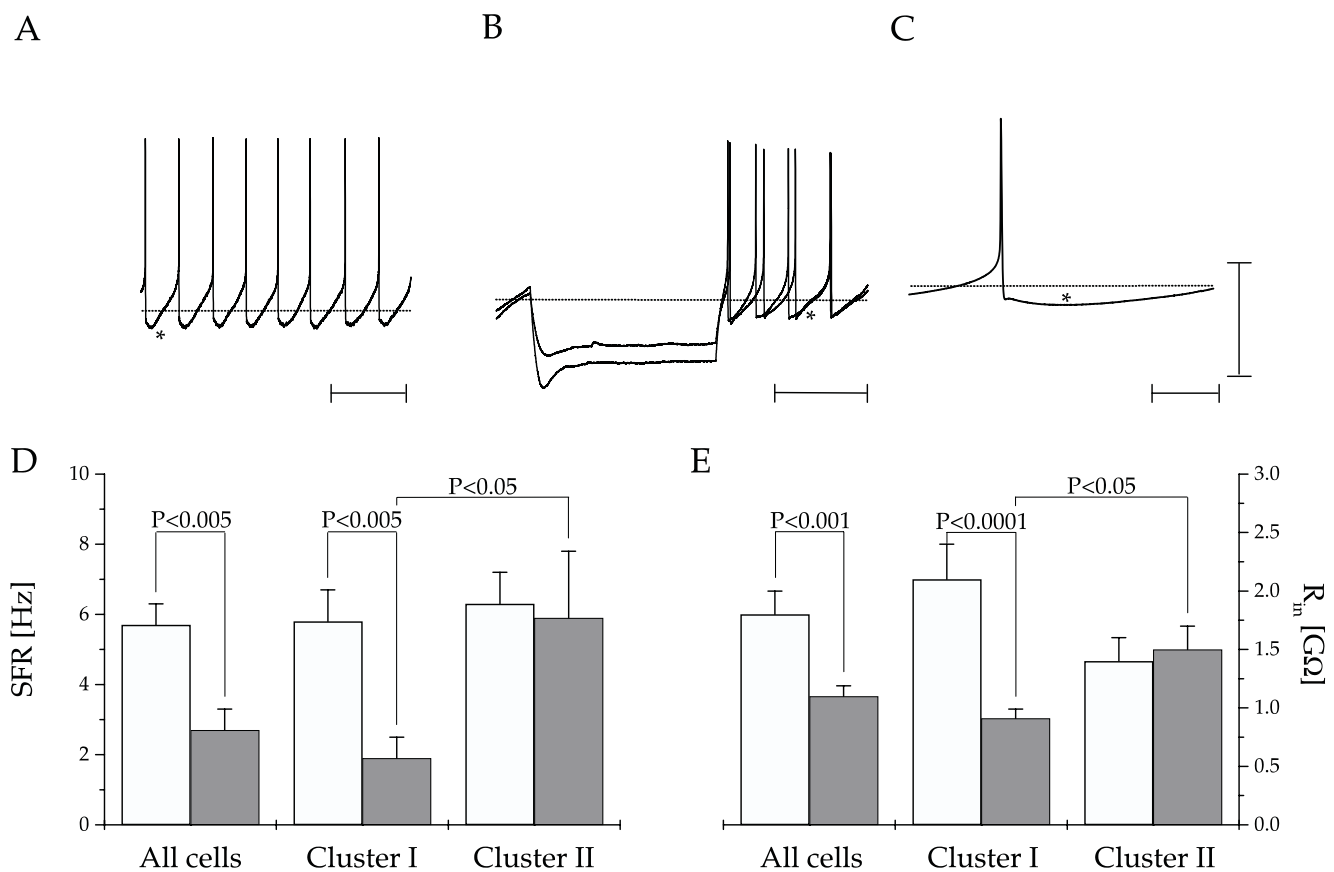

Fig. 5. Differences between cluster I and II cells: Spontaneous firing rate (SFR) and input resistance (R_{in}) during subjective day and night (data from experiment 3). (A) Example of spontaneous firing behavior of a cluster II cell. Note the high regularity of firing and slow spike afterhyperpolarization (asterisk). The SFR during this recording was 4.7 Hz and the basal membrane potential was −65 mV (dotted line). (B) Example of voltage responses to hyperpolarizing current steps of −25 and −35 pA. The R_{in} was 0.97 GΩ and the MP −58 mV. (C) Example of cluster II spike waveform. An average of 74 spontaneously generated spikes is shown. The slow, biphasic spike afterhyperpolarization is clearly visible. For clustering criteria, see Section 2 or Ref. [22]. Horizontal scale bars denote (A,B) 500 ms and (C) 50 ms, whereas the vertical scale bar represents 50 mV. The circadian difference in SFR and R_{in} of the total population and cluster I and II cells is shown in the lower panels with (D) the SFR and (E) the R_{in}. Error bars denote s.e.m. Statistically significant differences are marked with a *P*-value calculated using Mann–Whitney's *U*-test. Note the larger circadian differences between cluster I cells, whereas these differences were absent in cluster II cells. In the night period cluster II cells fired at significantly higher rates and exhibited a higher input resistance than cluster I cells. Sample sizes were: cluster I, day: $n = 16$, night: $n = 21$; cluster II, day: $n = 6$, night: $n = 4$.

ysis. It turned out that pipettes could be reused for up to 6 subsequent loose-patch recordings.

The third series differed from the first one only in its temporal aspect. In this series the spontaneous firing rate was measured for one minute immediately after rupturing the membrane. Subsequently voltage responses to hyperpolarizing and depolarizing current steps were recorded.

In order to assess day/night differences in circadian rhythmicity among an immunocytochemically characterized subpopulation in the SCN some neurons were recorded with biocytin-loaded pipettes (5 mM biocytin; otherwise the solution was the same as noted above). Neurons recorded with biocytin in the pipette were measured only for one or two minutes to minimize dialysis of cellular contents and associated changes in membrane properties. This short recording duration limited our analysis of these cells to only two membrane properties, viz. MP and SFR. Staining methods were as described before [26]. Briefly, following termination of the experiment, slices were fixed in 4% paraformaldehyde in 100 mM phosphate buffer (pH 7.4) for 30 h. After fixation slices were rinsed in Tris buffered saline (TBS; 50 mM Tris buffer and 150 mM NaCl at pH 7.4–7.6) and incubated overnight at 4°C with rabbit neurophysin antiserum (1:2000; kindly provided by Dr. A.G. Robinson, University of Pittsburgh, USA) in TBS containing 0.25% gelatin and 0.5% Triton X-100. After rinsing in TBS, slices were incubated in donkey anti-rabbit-FITC (1:200) for labeling of neurophysin and streptavidin-CY3 (1:1000) for biocytin. Following a final wash in TBS, slices were mounted on gelatin-coated slides and coverslipped with Vectashield® (Vector Laboratories). Using a Zeiss confocal laser scanning microscope equipped with lasers emitting at 488 and 543 nM, FITC and CY3 were visualized. Neurophysin is the precursor peptide of

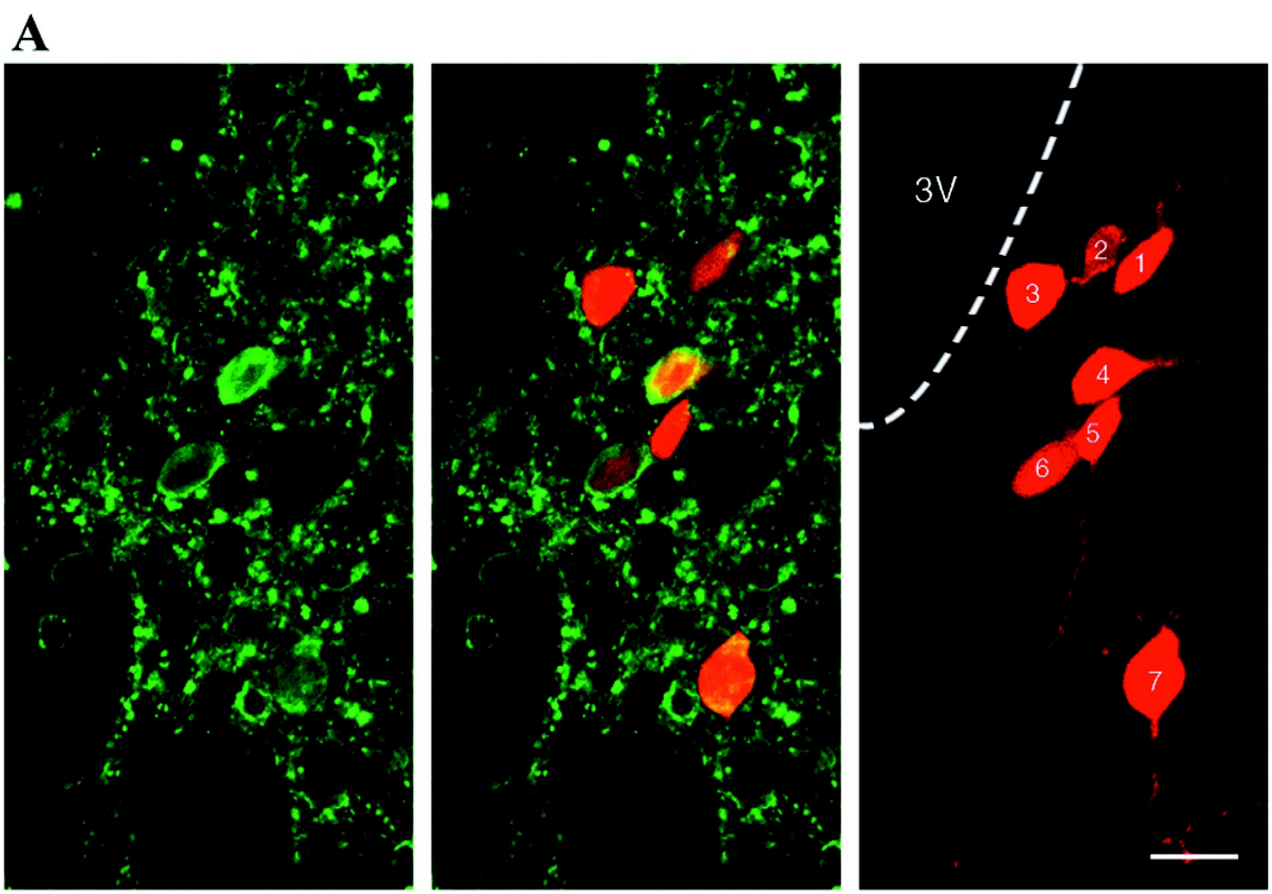

Fig. 6. Recordings from the vasopressin neurons in the SCN, assessed directly after membrane rupture. (A) Identification of vasopressin neurons by double labeling with biocytin and neurophysin antibody. Because the position of these cells was noted in an overview sketch of the slice, a particular set of whole-cell recordings could be assigned to each labeled neuron. In the right panel, 7 neurons (marked 1–7) are shown that were successfully injected with biocytin during whole-cell recording (red). In the left panel the immunocytochemical staining for neurophysin is shown (green). Overlay of the left and right panel (middle panel) combined with direct comparison between the left and right panel, indicate that cell number 1–3 and 5 are VP-negative, whereas cells 4, 6 and 7 are VP-positive. Scale bar: 20 μm, 3V: third ventricle. (B,C) Representative examples of whole-cell recordings from VP-positive cells. Immediately after break-in, recordings from limited duration were made, providing data on SFR and MP. Voltage traces of recordings during subjective day (B) and night (C) are shown. Scale bars denote 500 ms (*x*-axis) and 50 mV (*y*-axis) while dotted lines denote the membrane potential, −53 mV (B, day) and −63 mV (C, night). Note the monophasic shape of spike afterhyperpolarization and the SFR, which is still irregular in spite of a high firing rate during daytime (12 Hz). (D, E) Circadian rhythmicity of the VP-positive neurons. Average values of both spontaneous firing rate (D) and basal membrane potential (E) ± s.e.m. are plotted for subjective day and night. The difference between CT 4–10 and CT 12–24 was significant according to Mann–Whitney's *U*-test: $P < 0.005$ for SFR and MP.

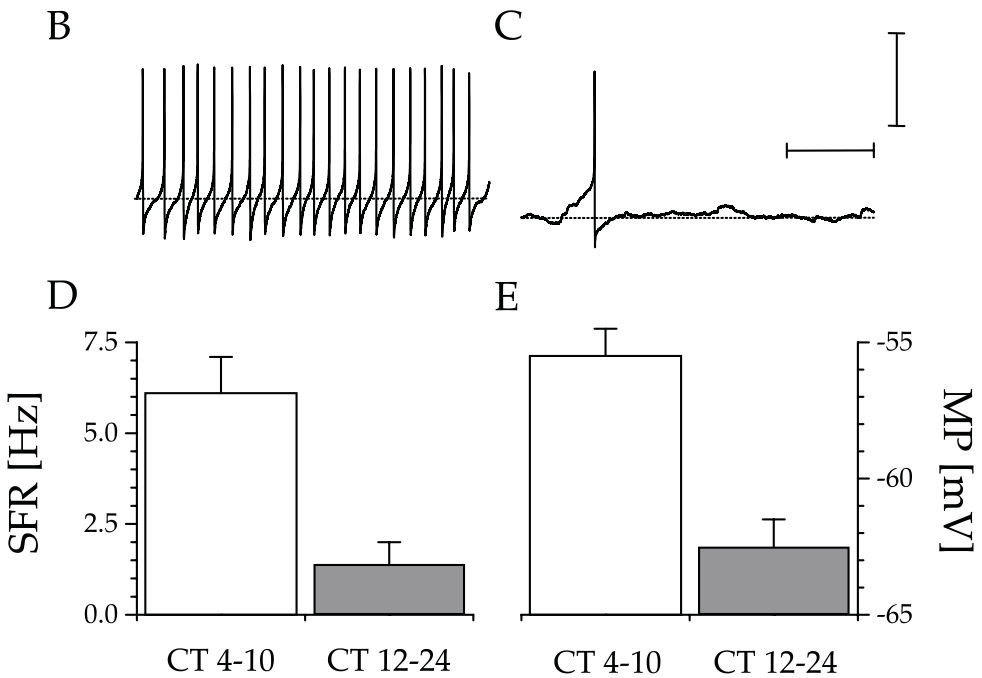

Fig. 6 (continued).

vasopressin and oxytocin. Because oxytocin is not expressed in SCN neurons, the neurophysin staining can be safely assumed to label vasopressin cells.

Cells were excluded from further analysis when the action potential amplitude, quantified with respect to the baseline, was less than 60 mV.

2.3. Data-analysis

Voltage responses to hyperpolarizing current were used to calculate the R_{in}. To correct for the slowly activating H-current (which underlies time-dependent inward rectification) the first few hundreds of milliseconds prior to visible manifestation of the H-current were fitted by a monoexponential function that produced both the τ_m and the predicted steady-state voltage response. These steady-state responses to sequential steps were plotted against the injected current and fitted by linear regression. The resulting slope was taken as the R_{in}, while the slope of the difference between measured and predicted voltage responses versus injected current served as a crude estimate of time-dependent inward rectification.

Evoked spike trains were used to estimate frequency adaptation and the magnitude of the ensuing AHP_T. The frequency adaptation was determined by calculating the slope of a linear fit through a plot of spike interval duration versus time relative to the start of the current step, which was 35 or 40 pA in amplitude. The most negative voltage attained during the spike train afterhyperpolarization relative to baseline was taken as a measure for AHP_T.

Recorded neurons were clustered according to the criteria of Pennartz et al. [22]. In short, the regularity of neuronal firing in the range of 1 to 5 Hz, the shape of the spike AHP, and the rebound depolarization directly following hyperpolarizing current injection served to classify cells as belonging to cluster I, II or III. The SFR was only used as a clustering criterion when it was in between 1 and 5 Hz. Whenever a cell was firing at a higher rate, hyperpolarizing current was injected in order to achieve firing within the desired range. Conversely, cells with a SFR lower than 1 Hz were depolarized to raise the firing rate between 1 and 5 Hz. This procedure allows to assess the regularity of firing with minimal dependence on the SFR. Cluster I cells were characterized by their irregular firing (coefficient of variation, CV, greater than 0.2; determined with $1 < SFR < 5$ Hz) and monoexponential shape of the spike AHP. Neurons were only classified as belonging to cluster II when the firing behavior was regular (CV < 0.2) and neurons displayed a slow, biphasic spike-afterhyperpolarization. Cluster III neurons were characterized by large rebound potentials (low-threshold Ca^{2+} spikes) occurring in response to hyperpolarizing current pulses of 30 pA or more.

All day–night differences were tested with Mann–Whitney's *U*-test but were generally equally significant with the Students' *t*-test. Correlations were computed using Spearman's Rank order correlation. These non-parametric tests were used because most membrane properties are not normally distributed [22]. Circadian time was estimated by extrapolating the light/dark regime in the animal housing facility.

3. Results

3.1. Experiment 1: prolonged whole-cell recordings

In the first experiment, whole-cell recordings from 109 cells were used to assess membrane properties after a period in which firing behavior was allowed to stabilize. This approach was initially taken because the SFR was seen to vary just after break-in. Cells were recorded throughout the SCN and care was taken to sample an approximately equal amount of cells over subjective day and night. A surprising observation was that the spontaneous firing rates during subjective day were very similar to those measured during subjective night, in contrast to our expectations [7,8,18]. Similarly, the R_{in}, τ_m, frequency adaptation and AHP_T showed no significant day/night differences. Although SCN cells tended to show stronger frequency adaptation during subjective night, the difference was not significant. Upon detailed analysis this tendency could be ascribed to a few cluster III cells at night exhibiting very strong frequency adaptation [22] (Table 1).

3.2. Experiment 2: cell-attached recordings

The results from Experiment 1 were contrary to our expectation in that at least the SFR should have been higher during subjective day as compared to night. Two explanations were considered to account for these findings, viz. that (i) our preparation procedure produced slices without rhythmicity or (ii) the circadian rhythm was lost as a consequence of the whole-cell procedure. To examine the functional preservation of circadian rhythmicity in our thin slice preparation a series of cell-attached voltage clamp measurements was started. This method allows for on-cell recording of action potentials without introducing further changes in methodology, except for a lower seal resistance and absence of membrane rupture and subsequent whole-cell dialysis. Examples of cell-attached current traces are shown in Fig. 1a–b. The SFR in cell-attached recordings was plotted against circadian time and a circadian pattern can be seen (Fig. 1c–d). The mean firing rate was significantly higher during subjective day than night (CT 4–10: 3.5 ± 0.6 Hz; CT 12–24: 1.4 ± 0.3 Hz; $P < 0.005$). This difference was in part due to the larger fraction of silent cells during the night. Thus, both our thin slice preparation and cell-approaching methods were suitable for measuring circadian rhythms. The combined findings of Experiments 1 and 2 also suggest that long-lasting whole-cell recordings compromise expression of circadian rhythmicity in SCN neurons.

3.3. Experiment 3: whole-cell recordings directly after membrane rupture

In a third experiment we tested the hypothesis that circadian rhythmicity would be gradually lost during whole-cell recording and would thus be present immediately after break-in. In this series both SFR and R_{in} were recorded within the first two minutes after break-in. Representative examples of SFR, hyper- and depolarizing traces are shown for subjective day and night (Fig. 2).

The day-time firing rate of the neurons in this series ($n = 51$) was significantly higher than during subjective night ($P < 0.001$; Fig. 3 and Table 2). This observation shows that in principle the whole-cell recording method is suitable for assessing circadian rhythms, provided that the measurements can be made within a short period after break-in. The R_{in} was clearly elevated during the subjective day (Fig. 4; $P < 0.001$). The circadian rhythm in R_{in} was roughly in phase with the rhythm in SFR (Figs. 3 and 4) which is in agreement with the positive correlation we found between SFR and R_{in} ($r = 0.41$; $P < 0.005$). These and other electrophysiological properties have been summarized in Table 2. Probably as a consequence of the lower SFR, the coefficient of variation was higher during the subjective night (Table 2; $P < 0.05$; cf. Ref. [22]).

The MP did not significantly differ across subjective day and night. However, we found a trend towards a higher MP during subjective daytime ($P < 0.15$), in agreement with a positive correlation between MP and SFR ($r = 0.41$; $P < 0.005$). The τ_m showed a significant day/night difference which was, however, not as clear-cut as that in R_{in}. τ_m and R_{in} were strongly correlated ($r = 0.58$; $P < 0.0001$), suggesting that at least part of the enhanced R_{in} during subjective day is due to an enhanced membrane resistance per unit of area, assuming a constant capacitance. Furthermore, the amount of time-dependent inward rectification quantified as explained in Section 2, was higher during the day as compared to night (subjective day: 0.59 ± 0.1 mV pA^{-1} ($n = 25$); night: 0.28 ± 0.07 mV pA^{-1} ($n = 23$); $P < 0.05$). Time-dependent inward rectification was strongly correlated to the R_{in} ($r = 0.60$; $P < 0.0001$), raising the possibility that this difference arose as a consequence of the higher voltage response during subjective day rather than through a circadian modulation of the H-current.

Finally, both the adaptation rate in spike trains and the spike-train afterhyperpolarization were significantly higher during subjective day than during night (Table 2). No difference in the number of spikes during the spike-train between subjective day and night could be detected. It is thus logical to propose that the observed day/night difference in frequency adaptation and AHP_T is not dependent on factors determining the mean firing rate during spike trains (e.g. R_{in}, MP and SFR).

Considering the different outcome of Experiments 1 and 3 regarding the circadian rhythm in SFR, we asked whether the SFR during the day was subject to a gradual decline within the first 5–8 min of recording (Tables 1 and 2). Indeed, we found that the SFR dropped from an initial value of 5.5 ± 0.8 Hz to 3.5 ± 0.6 Hz ($P < 0.02$, Wilcoxon's test, $n = 21$). Cells recorded during subjective

night did not reveal a significant decline in SFR during prolonged recordings.

Thus far we have only considered the overall population of SCN cells. Taking into account the large day/night differences in membrane properties measured shortly after break-in, it is essential to ask to what extent different cell clusters contribute to these differences. Cluster II cells, characterized by regular firing and a long-lasting, biphasic spike AHP (Fig. 5a–c), showed a similar SFR and R_{in} as cluster I cells during subjective day, but not during subjective night. In cluster II cells neither the SFR nor R_{in} exhibited a significant difference between subjective day and night, whereas cluster I cells showed more pronounced circadian rhythmicity as compared to the overall population (Figs. 3–5d–e).

By means of immunocytochemical staining, intracellularly recorded neurons were distinguished on the basis of their neurotransmitter content. Out of 86 neurons successfully labeled with biocytin, 32 cells were immunoreactive to the precursor peptide of VP, neurophysin. As reported elsewhere [21] these cells were characterized as belonging to cluster I. The vasopressin (VP) positive neurons appeared to express a particularly strong circadian rhythmicity (Fig. 6). Both SFR and MP were significantly higher during subjective day compared to night with larger day/night differences than shown by the total population of SCN neurons (subjective day SFR: 6.1 ± 1 Hz; MP: -55.5 ± 0.9 mV; night SFR: 1.4 ± 0.6 Hz; MP: -62.5 ± 1.1 mV; SFR: $P < 0.05$; MP: $P < 0.005$). These differences were partially due to the relatively large group of silent cells among the VP neurons during subjective night (53%) as compared to the total population (28% silent cells).

4. Discussion

No significant day/night differences were detected in whole-cell recordings from SCN neurons measured long after membrane rupture (Experiment 1). However, a circadian rhythm in SFR appeared to be present in cell-attached measurements (Experiment 2), indicating that our preparation preserved circadian rhythmicity and that physical disruptions associated with seal formation do not severely interfere with the assessment of this rhythmicity. Furthermore, circadian rhythmicity in SFR, R_{in}, τ_m, time-dependent inward rectification, frequency adaptation and spike train afterhyperpolarization was found in whole-cell measurements directly after break-in (Experiment 3).

4.1. Patch-clamp approaches for studying circadian rhythmicity

Since the whole cell recordings of the first experiment did not reveal significant differences between subjective day and night (Table 1) it was necessary to examine circadian rhythmicity using a less disruptive method, viz. cell-attached recording.

The cell-attached recordings of Experiment 2 showed a clear circadian variation in SFR. The plot of SFR versus time (Fig. 3) is qualitatively similar to the data published before [7,8] and also the ranges of firing rates resemble each other. However, a remarkable difference is the substantial amount of silent night cells (Experiment 2: 61%; Experiment 3: 28%, and 53% for vasopressin cells), in contrast to the extracellular recording technique which makes it difficult to take silent cells into account. Therefore the method of extracellular unit sampling underestimates the amplitude of the circadian rhythm in SFR.

In contrast to the whole-cell recordings of Experiment 1, membrane properties measured immediately after break-in (Experiment 3) did show a circadian rhythm in several parameters, including SFR. The observation that a circadian rhythm can be recorded in whole-cell mode until a few minutes after break-in shows that the expression of circadian rhythm is probably independent, at least to a considerable extent, of the maintenance of ionic transmembrane gradients. Namely, during whole-cell recording the ionic concentrations within the neuron become essentially clamped to the pipette solution which, of course, was held equal for subjective day and night recordings. Following membrane rupture, a novel equilibrium in $[Na^+]_i$, $[Cl^-]i$, $[K^+]_i$ and $[Ca^{2+}]_i$ is probably reached with a time constant in the order of 1 to 10 s [15,24], although diffusional exchange within dendrites may be somewhat slower. Therefore it appears unlikely that intraneuronally generated circadian alterations in transmembrane gradients of small ions constitute a mechanism underlying expression of circadian rhythmicity.

It could be argued that the absence of circadian rhythmicity in prolonged whole-cell recordings (Experiment 1), vis à vis its presence in short-term recordings (Experiment 3) does not demonstrate a gradual loss of circadian rhythmicity per se because these two sets of recordings were obtained from different groups of cells. However, our slice preparation and cell approach methods as well as the experimental setups used in Experiments 1 and 3 were virtually identical, making it difficult to ascribe the loss of circadian rhythmicity to changes in experimental conditions. Monitoring firing rates of a fixed set of cells across both initial and prolonged phases of recording is possible but not trivial, because several membrane properties such as action potential amplitude can be subject to changes over time [21]. When we followed a subset of neurons, sampled from subjective day and having constant spike characteristics across the first 4–8 min of recording, a decline in SFR as function of recording time was seen. This strengthens the proposition that a rundown of the circadian rhythmicity occurs in prolonged whole-cell recordings. Additional long-term recordings in a large number of cells would be needed to substantiate this conclusion further.

Two possible causes of the inferred rundown of the circadian rhythm in prolonged whole-cell recordings can be distinguished, viz. (i) a rundown of the general condition of the neuron by dialysis-induced changes in ionic conductances, and (ii) washout of specific cytoplasmic constituents (e.g. second messengers) controlling the expression of circadian rhythmicity. Because we only took into account recordings with spikes exceeding 60 mV, it is reasonable to argue that expression of circadian rhythmicity in prolonged whole-cell recordings was compromised while a severe rundown was absent. It would be worthwhile to examine this problem in further detail by adding constituents (e.g. ATP-regenerative system) to the patch-pipette fluid so that the cells can retain their metabolic status more optimally [15,24].

4.2. Circadian rhythmicity in electrophysiological properties

With whole-cell measurements directly after break-in, a circadian rhythm was shown to exist in several parameters, most prominently in SFR and R_{in} (Table 2, Figs. 3 and 4). Although the membrane potential tended to be more depolarized during daytime, this trend was not significant ($P < 0.15$). Nevertheless, the membrane potential was positively correlated to the SFR. Our results are largely in agreement with perforated patch studies which revealed day/night differences in SFR, R_{in} and MP [10]. Taking the latter results together with our findings on vasopressin neurons, which also showed a clear rhythm in MP, the balance of the overall results is inclined towards the presence rather than absence of a circadian rhythm in membrane potential (cf. Ref. [12]). That the corresponding day/night difference did not reach significance may be due to a large variability in membrane potential during the transitional phase of recording following break-in. Indeed, the observation of a clear day/night difference in the membrane potential of vasopressin cells may be ascribed to a selective focusing on one peptidergic phenotype of SCN neurons.

When comparing whole-cell recordings and perforated patch recordings in the context of studying circadian rhythmicity it should be recognized that the perforated patch method allows day/night differences to be studied across prolonged periods of recordings. On the other hand, whole-cell recordings offer the opportunity to label and subsequently stain recorded neurons and both success rate and number of recordings per unit of experimental time are enhanced. The rhythm in R_{in} presented here is roughly in phase with the rhythm in SFR (Figs. 3 and 4) in contrast to prior conductance measurements [12]. Although it is not clear at this point why Jiang et al. [12] found the rhythm in holding current and SFR versus R_{in} to be out of phase, a few suggestions to explain the discrepancy with our results can be given. First, despite a very large sample size, Jiang et al. [12] did not identify a significant circadian rhythm in SFR, in contrast to our study. Second, Jiang et al. [12] quantified the membrane conductance in a different way than was adopted here, viz. by holding the cell at -60 mV and measuring the instantaneous current response to a hyperpolarizing voltage step of 10 to 20 mV.

On account of their membrane properties different clusters of SCN neurons can be distinguished [22]. Our results indicated that cluster I cells express a strong circadian rhythm in SFR and R_{in} when measured shortly after break-in. In contrast, measurements in cluster II cells did not reveal a significant circadian rhythm in these or other properties. This lack of rhythmicity can be attributed to the fact that these cells were more active during the night as compared to cluster I cells. Thus, it can be tentatively concluded that cluster II cells do not prominently engage in expression of circadian rhythmicity, although larger sample sizes would be needed to substantiate this conclusion. As we measured no cluster III cells during subjective night, no conclusions can be drawn about their behavior. Vasopressin cells constitute a subpopulation of cluster I neurons as they display irregular firing behavior and a brief, monoexponential spike afterhyperpolarization [21]. They expressed a strong circadian rhythm in SFR and MP. While the pronounced day/night difference in the SFR of vasopressin cells is compatible with a prominent role of cluster I cells in the expression of rhythmicity, their rhythm in membrane potential was not generally found in cluster I cells. Therefore it can be argued that the approach of selectively studying one peptidergic phenotype can be favorable for identifying circadian modulation of membrane properties.

Block and coworkers proposed a model describing the coupling between presumably molecular clock processes intrinsic to basal retinal neurons of *Bulla gouldiana* with the membrane properties of those neurons [2,19]. In this model, an intracellularly driven rhythm in potassium conductance underlies a day/night cycle in MP and firing rate of basal retinal neurons. This scheme appears to be, at least in part, compatible with the data presented in this study. The higher input resistance during subjective day suggests the closure of as yet unidentified ionic channels. If these channels are assumed to be permeable to K^+ or Cl^-, their opening would result in membrane hyperpolarization, as was indeed observed to a modest extent in the overall population of neurons and more clearly in vasopressin neurons (cf. Ref. [10]). Thus, depending on the validity of this assumption, the *Bulla* model may fit the circadian modulation in R_{in}, τ_m, SFR and (in part) MP.

The circadian rhythm in membrane properties has several important functional implications. The conductances underlying frequency adaptation and AHP_T can be considered to contribute to the machinery by which SCN neurons regulate responses to synaptic events. GABA is considered to be the dominant neurotransmitter intrinsic to the SCN [5,20,29]. The SCN neurons have a higher firing rate during subjective day, leading to a higher incidence rate of GABAergic events. If GABAergic inputs are inhibitory,

the circadian rhythm in input resistance may help to delimit the firing rate of SCN neurons during daytime, because the effect that GABAergic input currents have on membrane potential will be amplified by a higher R_{in}.

Concurrent with the circadian rhythm in MP, R_{in}, τ_m and SFR we observed circadian modulation of frequency adaptation and AHP_T (Table 2). Frequency adaptation and spike-train afterhyperpolarizations with time constants in the order of 100 ms are likely to be caused by a Ca^{2+}-dependent K^+-current mediated by SK-channels [3,27,33]. It is important to note that the average number of spikes in the evoked spike trains was not different between subjective day and night (Table 2), arguing that the difference in frequency adaptation and AHP_T was not a secondary consequence of changes in basal membrane properties that can affect spike generation (e.g. MP, R_{in} and τ_m). Ionic currents underlying frequency adaptation are likely to modulate spike trains evoked by excitatory input, for instance photic signals relayed by the retina [12,14,32]. The response of SCN neurons to visual input has been reported to be larger during the subjective night when phase shifts can occur [17,18]. Ionic currents mediating frequency adaptation and AHP_T may contribute to the modulation of the excitatory retinal response by a stronger dampening of the evoked spike train during the subjective day.

5. Summary

In summary, the whole-cell patch-clamp method allows for investigation of circadian rhythmicity, but only during the first few minutes after break-in. With cell-attached patch and 'acute' whole-cell recording a circadian rhythm in spontaneous firing rate was demonstrated corresponding to results obtained with other recording methods. We found that the R_{in}, τ_m, frequency adaptation and AHP_T were higher during subjective day than during night. These findings suggest, on the one hand, a net reduction of basal ionic current flow and, on the other hand, an enhancement of Ca^{2+}-dependent K^+ current during daytime. Furthermore, vasopressin cells were also significantly hyperpolarized at night, relative to the day phase.

The circadian rhythm in spontaneous firing rate is accompanied by parallel changes in multiple membrane properties, suggesting a circadian modulation of several as yet unidentified conductances. In addition, immunocytochemically and electrophysiologically defined subpopulations of the suprachiasmatic neurons can exhibit more pronounced circadian modulation of membrane properties than applies to the overall population.

Acknowledgements

This study was supported by the Foundation Life Sciences grant no: 33.261.

References

[1] T. Akasu, S. Shoji, H. Hasuo, Inward rectifier and low-threshold calcium currents contribute to the spontaneous firing mechanism in neurons of the rat suprachiasmatic nucleus, Pflügers Arch. 425 (1993) 109–116.
[2] G.D. Block, S.B.S. Khalsa, D.G. McMahon, S. Michel, M. Guesz, Biological clocks in the retina: cellular mechanisms of biological timekeeping, Int. Rev. Cyt. 146 (1993) 83–143.
[3] C.W. Bourque, D.A. Brown, Apamin and D-tubocurarine block the afterhyperpolarization of rat supraoptic neurosecretory neurons, Neurosci. Lett. 82 (1987) 185–190.
[4] Y. Bouskila, F.E. Dudek, Neuronal synchronization without calcium-dependent synaptic transmission in the hypothalamus, Proc. Natl. Acad. Sci. USA 90 (1993) 3207–3210.
[5] R.M. Buijs, Y.X. Hou, S. Shinn, L.P. Renaud, Ultrastructural evidence for intra- and extranuclear projections of GABAergic neurons of the suprachiasmatic nucleus, J. Comp. Neurol. 340 (1994) 381–391.
[6] M.U. Gillette, Cellular and biochemical mechanisms underlying circadian rhythms in vertebrates, Curr. Opin. Neurobiol. 7 (1997) 797–804.
[7] D.J. Green, R. Gillette, Circadian rhythm of firing rate recorded from single cells in the rat suprachiasmatic brain slice, Brain Res. 245 (1982) 198–200.
[8] G.A. Groos, J. Hendriks, Circadian rhythms in electrical discharge of rat suprachiasmatic neurones recorded in vitro, Neurosci. Lett. 34 (1982) 283–288.
[9] E.D. Herzog, M.E. Geusz, S.B.S. Khalsa, M. Straume, G.D. Block, Circadian rhythms in mouse suprachiasmatic nucleus explants on multielectrode plates, Brain Res. 757 (1997) 285–290.
[10] M.T.G. de Jeu, M.L.H.J. Hermes and C.M.A. Pennartz, Circadian modulation of membrane properties in slices of rat suprchiasmatic nucleus, Neuroreport, in press.
[11] M.T.G. de Jeu, C.M.A. Pennartz, Functional characterization of the H-current in SCN neurons in subjective day and night: a whole-cell patch-clamp study in acutely prepared brain slices, Brain Res. 767 (1997) 72–80.
[12] Z.G. Jiang, Y.Q. Yang, Z.P. Liu, C.N. Allen, Membrane properties and synaptic inputs of suprachiasmatic nucleus neurons in rat brain slices, J. Physiol. 499 (1997) 141–159.
[13] Y.I. Kim, F.E. Dudek, Intracellular electrophysiological study of suprachiasmatic neurons in rodents: inhibitory synaptic mechanisms, J. Physiol. 458 (1992) 247–260.
[14] Y.I. Kim, F.E. Dudek, Membrane properties of rat suprachiasmaitc nucleus neurons receiving optic nerve input, J. Physiol. 464 (1993) 229–243.
[15] A. Marty and E. Neher, Tight-seal whole-cell recording, in B. Sakmann and E. Neher (Eds.), Single-Channel recording, 2nd ed., Plenum Press, New York, 1995, Ch. 2, p. 45.
[16] J.H. Meijer, W.J. Rietveld, Neurophysiology of the suprachiasmatic circadian pacemaker in rodents, Physiol. Rev. 69 (1989) 671–707.
[17] J.H. Meijer, B. Rusak, G. Gänshirt, The relation between light-induced discharge in the suprachiasmatic nucleus and phase shifts of hamster circadian rhytms, Brain Res. 598 (1992) 257–263.
[18] J.H. Meijer, K. Watanabe, L. Détàri, J. Schaap, Circadian rhythm in light response in suprachiasmatic nucleus neurons of freely moving rats, Brain Res. 741 (1996) 352–355.
[19] S. Michel, M.E. Geusz, J.J. Zaritsky, G.D. Block, Circadian rhythm in membrane conductance expressed in isolated neurons, Science 259 (1993) 239–241.
[20] R.Y. Moore, J.C. Speh, GABA is the principal neurotransmitter of the circadian system, Neurosci. Lett. 150 (1993) 112–116.
[21] C.M.A. Pennartz, N.P.A. Bos, M.T.G. de Jeu, A.M.S. Geurtsen, M. Mirmiran, A.A. Sluiter and R. M. Buijs, Membrane properties and morphology of vasopressin neurons in slices of rat suprachiasmatic nucleus, J. Neurophysiol. (1998) in press.

[22] C.M.A. Pennartz, M.T.G. de Jeu, A.M.S. Geurtsen, A.A. Sluiter, M.L.H.J. Hermes, Electrophysiological and morphological heterogeneity of neurons in slices of rat suprachaismatic nucleus, J. Physiol. 506 (1998) 775–793.
[23] R. Penner, A practical guide to patch-clamping, in: B. Sakmann and E. Neher (Eds.), Single-Channel recording, 2nd ed., Plenum Press, New York, 1995, Ch. 2, p. 8.
[24] M. Pusch, E. Neher, Rates of diffusional exchange between small cells and a measuring pipette, Pflügers Arch. 411 (1988) 204–211.
[25] R.M. Ralph, R.G. Foster, F.C. Davis, M. Menaker, Transplanted suprachiasmatic nucleus determines circadian period, Science 247 (1990) 975–978.
[26] H.J. Romijn, A.A. Sluiter, C.W. Pool, J. Wortel, R.M. Buijs, Differences in colocalization between FOS and PHI, GRP, VIP and VP neurons of the rat suprachiasmatic nucleus after a light stimulus during the phase delay versus the phase advance period of the night, J. Comp. Neurol. 372 (1996) 1–8.
[27] P. Sah, Ca^{2+}-activated K^{+} currents in neurones: types, physiological roles and modulation, Trends Neurosci. 19 (1996) 150–154.
[28] W.J. Schwartz, R.A. Gross, M.T. Morton, The suprachiasmatic nuclei contain a tetrodotoxin-resistant circadian pacemaker, Proc. Natl. Acad. Sci. USA 84 (1987) 1694–1698.
[29] G.J. Strecker, J.-P. Wuarin, F.E. Dudek, GABA-A mediated local synaptic pathways connect neurons in the rat suprachiasmatic nucleus, J. Neurophysiol. 78 (1997) 2217–2220.
[30] J.S. Takahashi, Circadian-clock regulation of gene expression, Curr. Opin. Gen. Dev. 3 (1993) 301–309.
[31] D.K. Welsh, D.E. Logthetis, M. Meister, S.M. Reppert, Individual neurons dissociated from rat suprachiasmatic nucleus express independently phased circadian firing rhythms, Neuron 14 (1995) 697–706.
[32] H.V. Wheal, A.M. Thomson, The electrical properties of neurones of the rat suprachiasmatic nucleus recorded intracellularly in vitro, Neuroscience 13 (1984) 97–104.
[33] L. Zhang, C.J. McBain, Potassium conductances underlying repolarization and afterhyperpolarization in rat CA1 hippocampal interneurones, J. Physiol. 488 (1995) 661–672.